

Geometric Correlations and Breakdown of Mesoscopic Universality in Spin Transport

İ. Adagideli,¹ Ph. Jacquod,² M. Scheid,³ M. Duckheim,⁴ D. Loss,⁵ and K. Richter³

¹*Faculty of Engineering and Natural Sciences, Sabanci University, Orhanli-Tuzla, 34956 Istanbul, Turkey*

²*Physics Department, University of Arizona, 1118 E. 4th Street, Tucson, Arizona 85721, USA*

³*Institut für Theoretische Physik, Universität Regensburg, D-93040 Regensburg, Germany*

⁴*Dahlem Center for Complex Quantum Systems, Freie Universität Berlin, 14195 Berlin, Germany*

⁵*Department of Physics, University of Basel, CH-4056 Basel, Switzerland*

(Received 25 August 2010; published 10 December 2010)

We construct a unified semiclassical theory of charge and spin transport in chaotic ballistic and disordered diffusive mesoscopic systems with spin-orbit interaction. Neglecting dynamic effects of spin-orbit interaction, we reproduce the random matrix theory results that the spin conductance fluctuates universally around zero average. Incorporating these effects into the theory, we show that geometric correlations generate finite average spin conductances, but that they do not affect the charge conductance to leading order. The theory, which is confirmed by numerical transport calculations, allows us to investigate the entire range from the weak to the previously unexplored strong spin-orbit regime, where the spin rotation time is shorter than the momentum relaxation time.

DOI: 10.1103/PhysRevLett.105.246807

PACS numbers: 73.23.-b, 72.25.Dc, 85.75.-d

At low temperatures, linear electric transport properties of complex mesoscopic systems are statistically determined by the presence of a few symmetries only, most notably time-reversal and spin rotational symmetry [1,2]. This character of universality is believed to be independent of the source of scattering in the system, and to exist in both ballistic chaotic quantum dots and diffusive disordered conductors [3]. Universality in electric transport holds not only for global properties such as the conductance, but also for correlators of transmission amplitudes between individual channels. Thus, it is natural to expect that all transport properties that depend solely on the scattering matrix are universal as well. This conjecture has been theoretically verified for all charge transport properties, under the sole assumption that scattering generates complete ergodicity. Inspired by Ref. [4], several recent theoretical works [5–7] have further suggested that spin transport in mesoscopic systems with spin-orbit interaction (SOI) also displays universal random matrix theory (RMT) behavior. The agreement between numerics on the spin Hall conductance fluctuations in disordered systems [8] and the RMT prediction [4] seems to corroborate this conclusion.

In this work, we go beyond the conventional semiclassical theory of transport and show that even when all requirements for universality are met and the fluctuations of the spin and charge conductance as well as average charge conductance remain universal, the average spin conductance (SC) is finite in disagreement with RMT [4,6,7]. This effect originates from the SOI through which the electron spin perturbs the electron dynamics in such a fashion that, certain dynamical correlations survive despite the self-averaging nature of ergodic dynamics. These correlations depend on the geometry of the system, namely, the relative positions of the leads connecting the system to

external electronic reservoirs and the form of the SOI. Focusing on a two-dimensional quantum dot with Rashba SOI [9], we find that the average two-terminal SC G^μ in direction $\mu = x, y, z$ is proportional to $(\hat{\mathbf{z}} \times \mathbf{R})_\mu$. Here the vector \mathbf{R} connects the two terminals and $\hat{\mathbf{z}}$ is the unit vector perpendicular to the dot. This is illustrated in Fig. 1(a). The polarization of the average spin current is thus determined by the direction of the average electronic flow. In bulk diffusive systems, when the mean free path ℓ_d is shorter than the spin rotation length, this effect reduces to the extraction of the current-induced spin accumulation

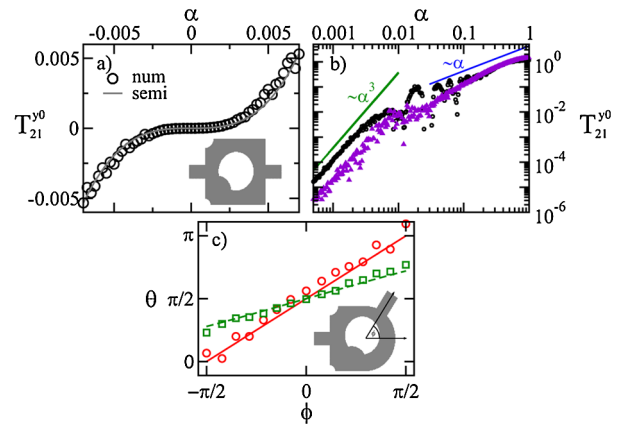


FIG. 1 (color online). Spin-dependent transmission coefficients \mathcal{T}_{21}^{y0} , Eq. (1), for (a) weak and (b) extended range of SOI showing the crossover from cubic (green line) to linear (blue line) behavior for the two-terminal chaotic quantum dot shown in the inset of panel (a). (c) Spin current polarization angle $\theta = \arctan(\mathcal{T}_{21}^{y0}/\mathcal{T}_{21}^{x0})$, for the system shown in the inset, where the right lead encloses an angle of ϕ with the x axis in the linear (squares) and the cubic (circles) regimes.

(CISA) and the spin Hall effect (SHE) [10–12] in finite systems. We stress, however, that the consequences of these geometric correlations have been considered in neither charge nor spin transport in quantum dots. Moreover, our calculations extend the existing theory for CISA and SHE in finite diffusive systems to the strong SOI regime (i.e., ℓ_d is longer than the spin rotation length). It is of practical importance to point out that the process that leads to finite SC is robust against temperature smearing or dephasing. From the point of view of mesoscopic spintronics, this opens up possibilities towards an electrically controlled generation and detection of pure spin currents, since the uncontrolled mesoscopic fluctuations of Refs. [4,6,7] are suppressed by simply raising the temperature.

We consider a mesoscopic quantum dot with no particular spatial symmetry as sketched in the insets of Fig. 1. We treat impurity and boundary scattering on equal footing and consider diffusive as well as ballistic chaotic charge dynamics. The dot is connected to two external leads. For simplicity, we assume idealized reflectionless leads in which the SOI vanishes. The realistic case of finite SOI in the leads can then be obtained by combining the scattering matrices of the realistic leads with that of the quantum dot. This choice allows us to uniquely define transport spin currents through a cross section of the leads without the ambiguities that plagued bulk calculations [13]. The leads are maintained at different electrochemical potentials eV_i , but have no spin accumulation. The scattering approach to transport gives the two-terminal SC as $G^\mu = \frac{e}{4\pi} \mathcal{T}_{21}^{\mu 0}$. Here the spin-dependent transmission coefficients $\mathcal{T}_{ij}^{\mu\nu}$ are obtained by summing over all transport channels in leads i and j [4,7],

$$\mathcal{T}_{ij}^{\mu\nu} = \sum_{m \in i, n \in j} \text{tr}[t_{mn}^\dagger \sigma_\mu t_{mn} \sigma_\nu], \quad \mu, \nu = 0, x, y, z. \quad (1)$$

Here, σ_μ are Pauli matrices (σ_0 is the identity matrix) and the trace is taken over the spin degree of freedom. The transmission amplitudes in Eq. (1) can be expressed in terms of the Green's function [14]. Next, we obtain the full Green's function $G^R(\mathbf{r}, \mathbf{r}')$ by either (i) the conventional Born approximation for impurity scattering inside the conductor or (ii) by a multiple reflection expansion for boundary scattering [15,16]. In case (ii), $G^R(\mathbf{r}, \mathbf{r}')$ is expressed as an iterative solution of

$$G^R(\mathbf{r}, \mathbf{r}') = G_0^R(\mathbf{r}, \mathbf{r}') - 2 \int d\alpha \partial G_0^R(\mathbf{r}, \boldsymbol{\alpha}) G^R(\boldsymbol{\alpha}, \mathbf{r}'), \quad (2)$$

where $\partial G_0^R(\mathbf{r}, \boldsymbol{\alpha}) = \hat{\mathbf{n}}_\alpha \cdot \nabla G_0^R(\mathbf{r}, \mathbf{x})|_{\mathbf{x}=\boldsymbol{\alpha}}$, with $\hat{\mathbf{n}}_\alpha$ the (inner) unit normal vector at the boundary point $\boldsymbol{\alpha}$. Finally, we evaluate the surface integrals in Eq. (2) asymptotically as $k_F L \rightarrow \infty$, where k_F is the Fermi wave number and L is the linear size of the conductor [16]. We obtain

$$\mathcal{T}_{ij}^{\mu 0} = \int_i dy \int_j dy_0 \sum_{\gamma, \gamma'} A_\gamma A_{\gamma'}^* e^{i(S_\gamma - S_{\gamma'})} \text{tr}[V_\gamma \sigma_\mu V_{\gamma'}^\dagger], \quad (3)$$

where the sums run over all trajectories γ starting at y_0 on a cross section of the injection lead and ending at y on the

exit lead. The classical action of γ is S_γ in units of \hbar and its stability is given by A_γ which includes a prefactor $(2\pi i \hbar)^{-1/2}$ as well as Maslov indices. For the spin-dependent part, we specialize to the Rashba SOI $H_R = (\hbar k_\alpha / m)(p_x \sigma_y - p_y \sigma_x)$, where k_α^{-1} is the spin precession length [9]. We then obtain

$$V_\gamma = \prod_{i=1}^{N_\gamma} V_{i,\gamma} = \prod_{i=1}^{N_\gamma} U_{i,\gamma} (1 + \delta U_{i,\gamma} + \xi \delta U_{i,\gamma}^{\text{hw}}), \quad (4)$$

$$\delta U_{i,\gamma} = \frac{k_\alpha}{4k_F} \left(\frac{\sin(k_\alpha |\mathbf{r}_i|)}{k_\alpha |\mathbf{r}_i|} - 1 \right) \boldsymbol{\eta} \cdot \hat{\mathbf{r}}_i, \quad (5)$$

$$\delta U_{i,\gamma}^{\text{hw}} = \frac{k_\alpha}{2k_F} \left(\frac{\sin(k_\alpha |\mathbf{r}_i|)}{k_\alpha |\mathbf{r}_i|} - 1 \right) \left(\boldsymbol{\eta} \cdot \hat{\mathbf{r}}_i - \frac{\boldsymbol{\eta} \cdot \hat{\mathbf{n}}_i}{\cos \theta_i} \right) + \frac{\sigma_z \sin \theta_i}{2k_F |\mathbf{r}_i| \cos \theta_i} [1 - \cos(k_\alpha |\mathbf{r}_i|)]. \quad (6)$$

Here $\xi = 0$ for a disordered system with weak, short-ranged impurities and $\xi = 1$ for a ballistic quantum dot with hard-wall confinement or a disordered system with strong, extended impurities. In both cases γ consists of segments $\mathbf{r}_i = (x_i, y_i, 0)$ with $i = 1, 2, \dots, N_\gamma$, $\hat{\mathbf{r}}_i = \mathbf{r}_i / |\mathbf{r}_i|$, $\hat{\mathbf{n}}_i$ is the (inner) unit normal vector and θ_i is the angle of incidence at the i th reflection point, $\boldsymbol{\eta} = \hat{\mathbf{z}} \times \boldsymbol{\sigma}$ and $U_{i,\gamma} = \exp[-ik_\alpha \boldsymbol{\eta} \cdot \mathbf{r}_i / 2]$ is the Rashba spin rotation matrix along segment i . We note that there are also corrections to A_γ which we have already ignored here, because they do not contribute to the SC. The Eqs. (3)–(6) fully describe spin and charge dynamics of coherent conductors.

The conventional semiclassical theory is obtained via the approximation $V_\gamma \approx \prod_{i=1}^{N_\gamma} U_{i,\gamma}$, which leads to the universal RMT predictions for charge transport [17,18]. We now show that this approximation also leads to RMT results for spin transport. We first start from the diagonal approximation, where $\gamma = \gamma'$, and obtain $\text{tr}[V_\gamma \sigma_\mu V_\gamma^\dagger] = 0$, showing that the diagonal contribution to the spin current vanishes. The next-order contributions within the conventional semiclassical theory of transport are the loop corrections, in which a self-crossing trajectory γ , is paired with a path γ' avoiding the crossing and going around the loop in the opposite direction [19,20]. Along the loop, γ' is the time-reversed of γ , and the loop contributions are proportional to $\langle \text{tr}[U_{\gamma_l} \sigma_\mu U_{\gamma_l}] \rangle$, where U_{γ_l} gives the spin rotation along the loop only. For a large SOI, U_{γ_l} is random, thus averaging produces vanishing weak localization correction to the SC. For a weaker SOI, we expand all spin rotation angles to second order in $k_\alpha L$ to obtain $\langle \text{tr}[U_{\gamma_l} \sigma_\mu U_{\gamma_l}] \rangle \approx 2i \delta_{\mu z} \langle \sin(k_\alpha^2 \delta \mathcal{A}_{\gamma_l}) \rangle$. The area difference $\delta \mathcal{A}_{\gamma_l}$ is given approximately by twice the directed area of the weak localization loop. For a chaotic system, the areas are symmetrically distributed around zero, thus the average vanishes. We note that extending the semiclassical approach of Ref. [21] to the calculation of the variance of the SC, one reproduces the leading-order RMT results of Ref. [4]. Details of this calculation will be presented elsewhere [16]. We conclude that conventional semiclassical theory, which

neglects effects of spin on the charge dynamics, only reproduces RMT predictions.

We next include the effects of SOI on the electronic dynamics and consider a two-dimensional conductor which can be either a ballistic quantum dot with hard-wall confinement, or a disordered system with short-ranged impurities. To do this, we go back to Eqs. (4)–(6) and include the corrections to the amplitude A and the spin matrix U to order $O(k_\alpha/k_F)$ and $O(1/k_F|\mathbf{r}_l|)$. We now assume that different trajectory segments are uncorrelated and define $\mathcal{U}_{l,\gamma} = \prod_{i=l+1}^{N_\gamma} U_{i,\gamma}$ to obtain

$$\langle \text{tr}[V_\gamma V_\gamma^\dagger \sigma_\mu] \rangle = \left\langle \sum_{l=1}^{N_\gamma} \text{tr}[\mathcal{U}_{l,\gamma} V_{l,\gamma} V_{l,\gamma}^\dagger \mathcal{U}_{l,\gamma}^\dagger \sigma_\mu] \right\rangle. \quad (7)$$

We see that spin currents have contributions from every trajectory segment, which are further rotated by the fluctuating spin-orbit fields of the subsequent reflections. We distinguish three different regimes that depend on the balance between linear system size L , the mean distance between (boundary or impurity) scatterings $\ell = \langle |\mathbf{r}_l| \rangle$, and SOI length k_α^{-1} : (i) the spin-ballistic small SOI limit $k_\alpha L$, $k_\alpha \ell \ll 1$, (ii) the spin-diffusive limit $k_\alpha \ell \ll 1 \ll k_\alpha L$, (iii) the spin-chaotic strong SOI limit $k_\alpha L$, $k_\alpha \ell \gg 1$. In regimes (i) and (iii), the orbital dynamics can be chaotic ballistic or diffusive depending on the ratio between ℓ and L . We will be focusing on long ergodic or diffusive trajectories γ for which we ignore the averages $\langle \sin\theta_i \rangle_\gamma$ and $\langle \hat{\mathbf{n}}_i \rangle_\gamma$ for all three regimes, save for the case of a quantum dot in regime (i) (see below).

In the *small SOI regime* (i), we expand the right-hand side of Eq. (7) to leading order in $k_\alpha \ell$ setting $\mathcal{U}_{l,\gamma} = 1$ and $1 - \sin(k_\alpha |\mathbf{r}_l|)/k_\alpha |\mathbf{r}_l| \simeq (k_\alpha |\mathbf{r}_l|)^2/6$ in Eqs. (5) and (6). We get

$$\langle \text{tr}[V_\gamma V_\gamma^\dagger \sigma_\mu] \rangle \simeq \frac{k_\alpha^3 (1 + 2\xi)}{6k_F} \left\langle \sum_{l=1}^{N_\gamma} |\mathbf{r}_l| (\hat{\mathbf{z}} \times \mathbf{r}_l)_\mu \right\rangle_\gamma. \quad (8)$$

We now perform the average $\langle \cdot \cdot \cdot \rangle_\gamma$ over the set of trajectories γ . Although individual \mathbf{r}_i are pseudorandom in length and direction, being generated by the cavity's chaotic dynamics, they satisfy $\sum_i \mathbf{r}_i^\gamma \simeq \mathbf{R}_{ij}$, where \mathbf{R}_{ij} is the γ -independent vector connecting the injection and exit terminal. We thus obtain $\langle \text{tr}[V_\gamma V_\gamma^\dagger \sigma_\mu] \rangle = C [k_\alpha^3 \ell (1 + 2\xi) / (3k_F)] (\hat{\mathbf{z}} \times \mathbf{R}_{ij})_\mu$. Here C is a number of order one that depends on geometric details of the cavity. This factor multiplies the independently averaged orbital terms in Eq. (3) for $\gamma = \gamma'$, which we compute as in, e.g., Ref. [20]. We estimate $\ell = \langle |\mathbf{r}_l| \rangle \simeq \pi \mathcal{A} / \mathcal{L}$ for a chaotic dot of area \mathcal{A} and perimeter \mathcal{L} , and $\ell = \ell_d$ for a diffusive system. We finally obtain

$$\langle \mathcal{T}_{ij}^{\mu 0} \rangle = C \frac{k_\alpha^3 \ell (1 + 2\xi)}{3k_F} (\hat{\mathbf{z}} \times \mathbf{R}_{ij})_\mu \times \begin{cases} \frac{N_i N_j}{N_T}, & \ell \geq L, \\ \frac{k_F W \ell}{L}, & \ell \ll L, \end{cases} \quad (9)$$

with the number $N_i = \text{Int}(k_F W_i / \pi)$ of channels in lead i , $N_T = \sum_i N_i$ and $W = \min W_i$ the width of the narrowest

lead. In the ballistic limit, this formula has an additional term $\frac{k_\alpha^3 \ell^2 \xi N_i N_j}{3k_F N_T^2} \sum_l N_l (\hat{\mathbf{z}} \times \hat{\mathbf{R}}_l)_\mu$, where \mathbf{R}_l is the average momentum direction of electrons entering through lead l , originating from nonzero $\langle \hat{\mathbf{n}}_i \rangle_\gamma$ [16]. We see that the average spin-dependent transmission, and thus the average spin currents, are determined by the relative position of the injection and exit lead and are proportional to the classical conductance from j to i .

In the *spin-diffusive case* (ii), $L \gg k_\alpha^{-1} \gg \ell$, the spins precess around randomly oriented SOI fields, thus relaxing via the Dyakonov-Perel mechanism. In particular, we can no longer set $\mathcal{U}_{l,\gamma} = 1$ in Eq. (7). Instead, we assume that γ is a stochastic sequence of segments with random orientations φ_i , which determine the spin rotation $U_{i,\gamma}$. The sequence of rotations is computed by averaging over φ_i . For a general Pauli spin matrix $\mathbf{s} \cdot \boldsymbol{\sigma}$ one has

$$\int \frac{d\varphi_i}{2\pi} U_{i,\gamma} \mathbf{s} \cdot \boldsymbol{\sigma} U_{i,\gamma}^\dagger = \cos^2(k_\alpha |\mathbf{r}_i|/2) \mathbf{s} \cdot \boldsymbol{\sigma} + (|\mathbf{r}_i|^2/2) \sin^2(k_\alpha |\mathbf{r}_i|/2) \times \boldsymbol{\eta} (\mathbf{s} \cdot \boldsymbol{\sigma}) \boldsymbol{\eta}. \quad (10)$$

This average is different for in-plane and out-of-plane polarization, which is the origin of the anisotropy of the Dyakonov-Perel spin-relaxation time. In our case, the generated spin is in-plane and the second term in Eq. (10) vanishes [22]. We have

$$\frac{\langle V_\gamma V_\gamma^\dagger \rangle - 1}{1 + 2\xi} \simeq - \left\langle \sum_{l=1}^{N_\gamma} e^{-k_\alpha^2 \ell v_F \tau_l} \frac{k_\alpha}{2k_F} \frac{k_\alpha^2 \ell}{6} \boldsymbol{\eta} \cdot \mathbf{r}_l \right\rangle_\gamma, \quad (11)$$

where we used $k_\alpha \ell \ll 1 \ll k_\alpha L$, approximated $|\mathbf{r}_i| \simeq \ell$, $\forall i$ and introduced the duration τ_l of the first l segments of γ . For each possible choice of l , the spin rotation thus separates into a spin independent piece for segments $1, \dots, l-1$, a spin generation piece on segment l , and spin-relaxation pieces on segments $l+1, \dots, N_\gamma$. Fixing the endpoint \mathbf{r}_l of segment l and summing over all possible γ we obtain that the SC is proportional to a product of (i) a diffusive probability $P(\mathbf{x}_l, \mathbf{x}_j)$ to go from the injection lead to \mathbf{r}_l , (ii) a spin generation factor $(1 + 2\xi) k_\alpha^3 \ell \boldsymbol{\eta} \cdot (\mathbf{x}_l - \mathbf{x}_{l'}) / 12k_F$ times the probability of ballistic propagation from \mathbf{x}_l to $\mathbf{x}_{l'}$, (iii) a diffusive probability to propagate from point $\mathbf{x}_{l'}$ to the exit lead times the probability that the spin survives this diffusion. Thus we have

$$\langle \mathcal{T}_{ij}^{\mu 0} \rangle \propto \epsilon_{3\mu\nu} \frac{k_\alpha^3 \ell}{k_F} \int d\mathbf{x}_l d\mathbf{x}_j d\mathbf{x}_{l'} P(\mathbf{x}_l, \mathbf{x}_j) (\mathbf{x}_l - \mathbf{x}_{l'})^\nu \times (1 + 2\xi) \frac{e^{-|\mathbf{x}_l - \mathbf{x}_{l'}|/\ell}}{2\pi |\mathbf{x}_l - \mathbf{x}_{l'}|} P(\mathbf{x}_l, \mathbf{x}_{l'}) e^{-k_\alpha |\mathbf{x}_{l'} - \mathbf{x}_j|}. \quad (12)$$

Since the length scale characterizing $P(\mathbf{x}_l, \mathbf{x}_j)$ is L , we evaluate the integrals above asymptotically in the limit $k_\alpha \ell \ll 1 \ll k_\alpha L$. After some algebra we finally obtain

$$\langle \mathcal{T}_{ij}^{\mu 0} \rangle \propto \text{sgn}(k_\alpha) (1 + 2\xi) \frac{k_\alpha^2 \ell^2 W}{L^2} (\hat{\mathbf{z}} \times \mathbf{R}_{ij}), \quad (13)$$

up to a factor of order unity depending on details of how the leads (with width W) are attached to the cavity. Noting that for our geometry \mathbf{R}_{ij} is in the direction of the current flow and its magnitude is L , we obtain that the spin conductivity is $\sigma_s \propto ek_\alpha^2 \ell^2$ in agreement with the spin diffusion equation calculations [10,12].

Spin chaos regime (iii).—Similar to regime (ii), we average over uncorrelated direction angles θ_i but do not Taylor expand $\sin(k_\alpha |\mathbf{r}_l|)/k_\alpha |\mathbf{r}_l| - 1$. We instead take the average over the segment lengths $|\mathbf{r}_l|$ as $\prod_{i=l+1}^{N_\gamma} \langle \cos^2(k_\alpha |\mathbf{r}_i|/2) \rangle \approx 2^{N_\gamma - l}$ in a chaotic or stochastic system with $k_\alpha L \gg 1$. Equation (11) is then replaced by

$$\frac{\langle V_\gamma V_\gamma^\dagger \rangle - 1}{1 + 2\xi} = \left\langle \sum_{l=1}^{N_\gamma} 2^{l-N_\gamma} \frac{k_\alpha}{2k_F} \left(\frac{\sin(k_\alpha |\mathbf{r}_l|)}{k_\alpha |\mathbf{r}_l|} - 1 \right) \boldsymbol{\eta} \cdot \hat{\mathbf{r}}_l \right\rangle_\gamma.$$

Averaging over γ we see that the dominant contribution is the last term. We thus approximate the sum by its last term, and take $k_\alpha |\mathbf{r}_{N_\gamma}| \approx k_\alpha L \gg 1$ to obtain $\langle V_\gamma V_\gamma^\dagger \rangle_\gamma = 1 + (C' k_\alpha / 2k_F) \boldsymbol{\eta} \cdot \hat{\mathbf{R}}_j$. Here C' is $(1 + 2\xi)$ times a constant of order unity that depends on the details of the scattering near the lead. We finally obtain the transmission coefficient

$$\langle \mathcal{T}_{ij}^{\mu 0} \rangle = C' \frac{k_\alpha}{2k_F} (\hat{\mathbf{z}} \times \hat{\mathbf{R}}_j)_\mu \times \begin{cases} N_i N_j / N_T & \ell \geq L, \\ k_F W \ell / L & \ell \ll L. \end{cases} \quad (14)$$

Equations (9), (13), and (14) are our main results. They show how a finite SC emerges from classical geometric correlations depending on the positions of the leads. These equations can be straightforwardly extended to Dresselhaus SOI by substituting $\hat{\mathbf{z}} \times \mathbf{Q} \rightarrow (Q_x, -Q_y, 0)$ for $\mathbf{Q} = \mathbf{R}_{ij}$ [Eqs. (9) and (13)] or $\mathbf{Q} = \mathbf{R}_j$ [Eq. (14)].

To check these predictions we performed quantum transport calculations for a tight-binding Hamiltonian [23] with Rashba SOI and evaluated the spin-resolved transmission probabilities between two leads as defined in Eq. (1) for both the chaotic and diffusive cases. We computed the transmission for chaotic cavities, shown as insets in Fig. 1, averaged over 2000 different configurations of the Fermi energy and the position and orientation of the central antidot. Panel (a) shows for the small $\alpha = ak_\alpha$ regime (i) that the numerically obtained \mathcal{T}_{21}^{y0} (circles) for the cavity in the inset agrees very well with the predicted cubic behavior, Eq. (9), (solid line) for $C = 1$. In panel (b) \mathcal{T}_{21}^{y0} is depicted for the same chaotic cavity (black circles) and for a square cavity with Anderson disorder (violet triangles) for the entire range from weak to strong SOI [regime (i) to (iii)] demonstrating the crossover from cubic to linear behavior according to Eqs. (9) and (14). In panel (c) we numerically confirm the predicted direction of the in-plane spin polarization $\theta = \arctan(\mathcal{T}_{21}^{y0} / \mathcal{T}_{21}^{x0})$ for regime (i) [dashed line, squares, Eq. (9)] and regime (iii) [solid line, circles, Eq. (14)] by rotating the right lead around the semicircle billiard shown in the inset.

In conclusion, we have presented a semiclassical calculation of spin transport in mesoscopic conductors which incorporates next-to-leading order corrections to the semiclassical Green's function. We showed that in contrast to RMT predictions, the average SC does not vanish, even if all the conventional conditions for universality are met. Our method, moreover, allowed us to investigate the strong SOI regime for finite diffusive systems for the first time, Eq. (14).

This work has been supported by the funds of the Erdal İnönü chair and by TUBA under Grant No. I.A/TUBA-GEBIP/2010-1 (I. A.), by NSF under Grant No. DMR-0706319 (P. J.) and by DFG within SFB 689 (M. S., K. R.). I. A. and P. J. thank the University of Regensburg, and P. J. thanks the Basel Center for Quantum Computing and Quantum Coherence for their hospitality.

-
- [1] B. L. Altshuler, JETP Lett. **41**, 648 (1985); P. A. Lee and A. D. Stone, Phys. Rev. Lett. **55**, 1622 (1985).
 - [2] C. W. J. Beenakker, Rev. Mod. Phys. **69**, 731 (1997).
 - [3] K. B. Efetov, Adv. Phys. **32**, 53 (1983).
 - [4] J. H. Bardarson, İ. Adagideli, and Ph. Jacquod, Phys. Rev. Lett. **98**, 196601 (2007).
 - [5] Y. V. Nazarov, New J. Phys. **9**, 352 (2007).
 - [6] J. J. Krich and B. I. Halperin, Phys. Rev. B **78**, 035338 (2008); J. J. Krich, Phys. Rev. B **80**, 245313 (2009).
 - [7] İ. Adagideli, J. Bardarson, and Ph. Jacquod, J. Phys. Condens. Matter **21**, 155503 (2009).
 - [8] W. Ren *et al.*, Phys. Rev. Lett. **97**, 066603 (2006).
 - [9] E. I. Rashba, Sov. Phys. Solid State **2**, 1109 (1960).
 - [10] İ. Adagideli and G. E. W. Bauer, Phys. Rev. Lett. **95**, 256602 (2005).
 - [11] V. Sih *et al.*, Phys. Rev. Lett. **97**, 096605 (2006).
 - [12] İ. Adagideli *et al.*, New J. Phys. **9**, 382 (2007); Y. Tserkovnyak *et al.*, Phys. Rev. B **76**, 085319 (2007); M. Duckheim, D. L. Maslov, and D. Loss, Phys. Rev. B **80**, 235327 (2009); M. Duckheim *et al.*, Phys. Rev. B **81**, 085303 (2010).
 - [13] E. I. Rashba, Phys. Rev. B **68**, 241315 (2003).
 - [14] H. U. Baranger and A. D. Stone, Phys. Rev. B **40**, 8169 (1989).
 - [15] R. Balian and C. Bloch, Ann. Phys. (N.Y.) **60**, 401 (1970); **84**, 559 (1974).
 - [16] İ. Adagideli *et al.* (to be published).
 - [17] H. Mathur and A. D. Stone, Phys. Rev. Lett. **68**, 2964 (1992).
 - [18] O. Zeitsev, D. Frustaglia, and K. Richter, Phys. Rev. Lett. **94**, 026809 (2005).
 - [19] I. L. Aleiner and A. I. Larkin, Phys. Rev. B **54**, 14423 (1996).
 - [20] K. Richter and M. Sieber, Phys. Rev. Lett. **89**, 206801 (2002).
 - [21] P. W. Brouwer and S. Rahav, Phys. Rev. B **74**, 075322 (2006).
 - [22] We note that in more complicated geometries such as side contacts there will be out-of-plane spin polarization [10].
 - [23] M. Wimmer and K. Richter, J. Comput. Phys. **228**, 8548 (2009).